

Charging Time Characterization for Wireless RF Energy Transfer

Deepak Mishra, Swades De, and Kaushik R. Chowdhury

Abstract—Wireless energy transfer to the on-board energy storage element using dedicated radio frequency (RF) energy source has the potential to provide sustained network operation by recharging the sensor nodes on demand. To determine the efficiency of RF energy transfer (RFET), characterization of recharging process is needed. Different from classical capacitor-charging operation, the incident RF waves provide constant power (instead of constant voltage or current) to the storage element, which requires a new theoretical framework for analyzing the charging behavior. This work develops the charging equation for replenishing an energy-depleted storage element by RFET. Since the remaining energy on a sensor node is a random parameter, the RF charging time distribution for a given residual voltage distribution is also derived. The analytical model is validated through hardware experiments and simulations.

Index Terms—Wireless energy transfer; RF energy harvesting; constant power charging; charging time distribution

I. INTRODUCTION

In wireless sensor networks (WSNs), field sensors consume energy in sensing, storage, and communication of the sensed data. It is often difficult to access the deployed sensors to replace their batteries. Hence, quite a few recent research works have focused on realizing perennially operating sensor nodes by on-line replenishment of drained energy. Energy harvesting from the ambient sources like solar [1], vibration [2], wind [3], ambient radio frequency (RF) [4], and strain from human activities [5], are a few prominent ways to recharge a battery. But, as the availability of sufficient energy from the ambient sources cannot be guaranteed under all circumstances, these sources are unreliable for continuous network operation [6].

Dedicated (on demand) wireless energy transfer from a RF source is a potential solution to the ambient resource uncertainty [7]. However, the success of RFET relies on accurately predicting the charging efficiency and energy level after a finite charging duration. This is especially important in the integrated data and energy mule (IDEM) paradigm [8] that extends the concept of the conventional data mule [9]. An IDEM occasionally visits the field nodes, places itself nearby a node for collecting data wirelessly and recharging it via RFET. As the residual energy at a node is a random variable, there is a need to characterize the RF charging time distribution.

This work was supported by the Department of Electronics and Information Technology under grant number 13(2)/2012-CC&BT.

D. Mishra and S. De are with the Dept. Electrical Eng., IIT Delhi, New Delhi, India. E-mail: {deepak.mishra, swadesd}@ee.iitd.ac.in. K. R. Chowdhury is with the Dept. Electrical and Computer Eng., Northeastern University, Boston, MA, USA. E-mail: krc@ece.neu.edu.

Copyright (c) 2014 IEEE. Personal use of this material is permitted. However, permission to use this material for any other purposes must be obtained from the IEEE by sending an email to pubs-permissions@ieee.org

In [10], an optimal movement strategy of the mobile charger was proposed that minimizes the overall RF charging delay in the network. In [11], a joint energy-minimum routing and energy-balanced RF charging scheme for rechargeable WSNs was proposed. However, both of these works are based on simplified empirical linear charging model with a constant charging rate assumption. To our best knowledge, no analytical model is available in the literature to characterize RF charging time. Our developed RF charging model in the paper is aimed at filling this gap and providing a robust framework for analyzing the efficacy of the RF harvesting system with mobile chargers to provide sustainable network operation [8].

The problem of estimating the energy level during the charging operation (or the time to fully recharge the on-board storage) of a field sensor is non-trivial. To motivate the problem, we consider the energy storage element as a simple capacitor. In order to find the efficiency of dedicated RFET, characterization of charging time is required, which is different from the conventional charging of a capacitor from a constant voltage source, e.g., a DC power supply. In charging from a constant voltage source, the initial current is high and it asymptotically reduces to zero as the capacitor is charged up to the supply voltage. The voltage and current across an initially uncharged capacitor in a series RC circuit with V_0 as the supply voltage are respectively given as:

$$V_C(t) = V_0 \left[1 - e^{-\frac{t}{RC}} \right] \quad \text{and} \quad I(t) = \frac{V_0}{R} e^{-\frac{t}{RC}}.$$

The main difference between constant voltage charging and RF charging is that, *in the former the supply voltage is fixed, whereas the latter is a case of constant power charging, where the supply voltage increases and supply current decreases with the increase of voltage across the capacitor, because the power delivered to the load is constant.* Although the constant voltage charging equations are well known, there are very few analytical formulations on constant power charging. [12] provided the analytical solution for constant power loading of ultra-capacitors. It is different from our work in that, it is on constant power discharging rather than constant power charging. [13] derived an analytical expression for cell (source) voltage for constant power operation. However, it did not develop the charging time and capacitor voltage expressions, that are required for charging time characterization. To this end, in this work we develop analytical expressions for capacitor voltage, charging time in constant power charging, and charging time distribution as function of the residual voltage.

II. THE RF CHARGING PROBLEM

Here, the practical RF charging problem is outlined.

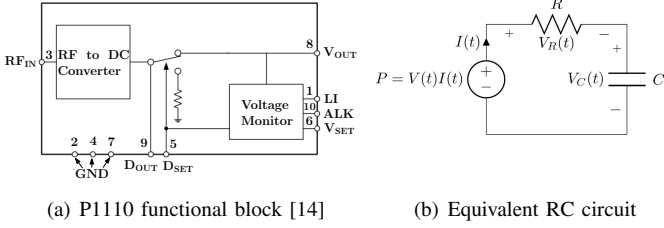


Fig. 1: RF charging module and equivalent circuit model

A. RF charging characteristics

Charging of a super-capacitor via dedicated RFET is a special case of constant power charging, as the RF power received for recharging the super-capacitor is fixed for a RF source transmitting constant power from a fixed distance. Consider the functional block of P1110 energy harvesting evaluation board in Fig. 1(a) [14] that operates at 915 MHz and harvests the RF input power in the range of -5 dBm to $+20$ dBm. It converts RF energy (radio waves) into DC power, which can be stored in a super-capacitor or used to directly power a circuit. Since the input power is constant, the charging current decreases as the voltage on the V_{OUT} pin increases. P1110 monitors the voltage on the storage element and turns off V_{OUT} when it is fully charged. The maximum output voltage from the harvester IC can be adjusted between 0 V or 4.2 V as per requirement. The equivalent series RC circuit model is shown in Fig. 1(b), where $V(t)$ is the voltage on V_{OUT} pin and P is the DC power available after rectification. RF charging time is analytically characterized in Section III, followed by the experimental validation in Section IV.

B. RF charging time distribution

Charging time depends on the residual energy of the node. So, the RF charging time can be represented as a function of residual voltage across the super-capacitor before charging, which can be modeled as a random variable. Thus, in a way RF charging time is also a random variable. RF charging time distribution for two example distributions of residual voltage are derived and validated by simulations in Section V.

III. ANALYTICAL MODELING OF RF CHARGING

For deriving the RF charging equations, the DC power available after RF to DC conversion by P1110 IC is modeled as constant power source with $V_{OUT} = V(t)$ as the source voltage and $I(t)$ as the source current with R as the equivalent series resistance (ESR) of the super-capacitor, C (cf. Fig. 1(b)).

A. Constant power charging equation

Applying Kirchhoff's voltage law in the circuit in Fig. 1(b),

$$\begin{aligned} V(t) &= V_R(t) + V_C(t) \\ P &= V(t) \cdot I(t) = [V_R(t) + V_C(t)] \cdot I(t) \\ &= R \cdot \left(\frac{dQ}{dt}\right)^2 + \frac{Q}{C} \cdot \frac{dQ}{dt}. \end{aligned} \quad (1)$$

Note that (1) is a first order, second degree, non-linear and non-homogeneous differential equation (DE) with Q as the dependent variable and t as the independent variable. Its explicit solution for Q cannot be obtained. We have solved it for T , the time required to store Q coulombs of charge in an uncharged capacitor, using the initial condition $Q(t=0) = 0$:

$$T = \frac{Q^2 + QA + 4C^2RP \ln\left(\frac{A+Q}{\sqrt{4C^2RP}}\right)}{4CP} \quad (2)$$

where $A = \sqrt{Q^2 + 4C^2RP}$. Call this solution as *method 1*.

As (1) cannot be solved for Q (and thus V_C and I) by solving DE, we take an alternative approach (*method 2*):

(1) is quadratic with $\frac{dQ}{dt}$ as the unknown. Its solution is:

$$\frac{dQ}{dt} = \frac{-\frac{Q}{C} + \sqrt{\left(\frac{Q}{C}\right)^2 + 4RP}}{2R}. \quad (3)$$

To solve for Q we integrate (3), where, as t goes from 0 to T , an initially uncharged capacitor charges up to Q Coulombs.

$$\int_0^T \frac{dt}{2R} = \int_0^Q \frac{dQ}{-\frac{Q}{C} + \sqrt{\left(\frac{Q}{C}\right)^2 + 4RP}}. \quad (4)$$

After simplifications, the solution for (4) is obtained as:

$$\begin{aligned} \frac{T}{2RC} &= \frac{1}{4} \ln \left[\frac{\sqrt{Q^2 + 4C^2RP} + Q}{\sqrt{Q^2 + 4C^2RP} - Q} \right] \\ &+ \frac{\sqrt{Q^2 + 4C^2RP}}{2(\sqrt{Q^2 + 4C^2RP} - Q)} - \frac{1}{2}. \end{aligned} \quad (5)$$

Using $A = \sqrt{Q^2 + 4C^2RP}$ and $Q = CV_C$ in (5), we get:

$$T = \frac{1}{2}RC \left[\frac{2CV_C}{A - CV_C} + \ln \left(\frac{A + CV_C}{A - CV_C} \right) \right]. \quad (6)$$

Expressions (2) and (6) obtained respectively by *methods 1* and *2* are equivalent, as demonstrated in Fig. 3(a). Also note that, T in (2) and (6) is a function of V_C .

Now, the RF charging voltage and current equations as a function of time t are derived. Let,

$$Z \triangleq \frac{\sqrt{Q^2 + 4C^2RP}}{\sqrt{Q^2 + 4C^2RP} - Q} \quad (7)$$

and replace T by t in (5), in order to find the voltage and current across an initially uncharged capacitor at any time t . Using (7) and simplifying, (5) can be expressed as:

$$(2Z - 1)e^{(2Z-1)} = e^{1 + \frac{2t}{RC}}. \quad (8)$$

(8) is of the form $ye^y = x$, which can be solved as $y = W(x)$, where $W(x)$ is the Lambert function [15]. For $x > 0$, the solution is denoted as $W_0(x)$ (principal branch). Thus, with the knowledge that $e^{1 + \frac{2t}{RC}} > 0$, (8) can be solved as:

$$Z = \frac{1}{2} \left[1 + W_0 \left(e^{1 + \frac{2t}{RC}} \right) \right]. \quad (9)$$

From (7), we have the solution for $Q(t)$ as:

$$Q(t) = \frac{2C\sqrt{RP}\left(1 - \frac{1}{Z}\right)}{\sqrt{1 - \left(1 - \frac{1}{Z}\right)^2}} \quad (10)$$

where Z is obtained from (9). Note that, in (10), Q has been replaced by $Q(t)$, because it denotes the charge on the capacitor at time t , and thus it is a function of t .

As $Q = CV_C$, the voltage across the capacitor at time t is:

$$V_C(t) = \frac{2\sqrt{RP}\left(1 - \frac{1}{Z}\right)}{\sqrt{1 - \left(1 - \frac{1}{Z}\right)^2}}. \quad (11)$$

From (3), the current across the capacitor at time t is:

$$I(t) = \frac{dQ}{dt} = \frac{-\frac{Q(t)}{C} + \sqrt{\left[\left(\frac{Q(t)}{C}\right)^2 + 4RP\right]}}{2R}. \quad (12)$$

B. Charging time distribution

RF Charging time T_C is defined as the time required to charge a super-capacitor from a residual value V' to a maximum allowable voltage V_H , which corresponds to the maximum energy that can be stored in the super-capacitor.

$$T_C = T(V_H) - T(V') \quad (13)$$

where $T(\cdot)$ is the RF charging time as derived in (6). It may be noted that V' is a random variable, with a lower limit bounded by V_L that corresponds to the minimum energy required in the super-capacitor for running the sensor node.

We have the cumulative distribution function (CDF) of T_C ,

$$\begin{aligned} F_{T_C}(t) &= P(T_C \leq t) = P[T(V_H) - T(V') \leq t] \\ &= P[T(V') > T(V_H) - t] \\ &= P\left[V' > \frac{2\sqrt{RP}\left(1 - \frac{1}{Z'}\right)}{\sqrt{1 - \left(1 - \frac{1}{Z'}\right)^2}}\right] \quad (\text{using (11), (6)}) \\ &= 1 - F_{V'}(v) \end{aligned} \quad (14)$$

where v is the initial residual voltage,

$$v = \frac{2\sqrt{RP}\left(1 - \frac{1}{Z'}\right)}{\sqrt{1 - \left(1 - \frac{1}{Z'}\right)^2}} \text{ with } Z' = \frac{1 + W_0\left(e^{1 + \frac{2(T(V_H) - t)}{RC}}\right)}{2}. \quad (15)$$

Note, (14) is derived using (11), (6), because $T(V')$ is the time up to which an initially uncharged capacitor charges to V' , and $\frac{2\sqrt{RP}\left(1 - \frac{1}{Z'}\right)}{\sqrt{1 - \left(1 - \frac{1}{Z'}\right)^2}}$ is the voltage across the capacitor at time $T(V_H) - t$. Also (11) is a non-decreasing function of t .

From (14), probability density function (PDF) of T_C is:

$$\begin{aligned} f_{T_C}(t) &= \frac{dF_{T_C}}{dt} = -f_{V'}(v) \frac{dv}{dt} \\ &= f_{V'}(v) \left\{ \frac{1}{C} \sqrt{\frac{P}{RZ''}} \right\} \end{aligned} \quad (16)$$

where $f_{V'}(v)$ is the PDF of the residual voltage, v is defined in (15) and $Z'' = W_0\left(e^{1 + \frac{2(T(V_H) - t)}{RC}}\right)$.

IV. EXPERIMENTAL VALIDATION

We have undertaken systematic experiments to validate the voltage and current across the super-capacitor as derived in (11) and (12), which we describe in this section.

A. Experimental setup and hardware system parameters

- 1) *RF source*: A HAMEG RF synthesizer HM8135 was used as the RF source that transmits at a power of +13 dBm via 6.1 dBi antenna at 915 MHz frequency.
- 2) *Receiver node*: Receiver node placed at a distance of 0.45 m from RF source consists of a P1110 evaluation board [14] that harvests the input power received from the source via 6.1 dBi antenna and converts it to DC. The evaluation board also consists of a 5.5 V 50 mF super-capacitor to store the converted DC energy.
- 3) *Digital meters*: Agilent multimeter 34405A was used to record the current samples into the super-capacitor after every 0.1714 s. These samples were stored in excel file using NI LabVIEW. The voltage across the super-capacitor was measured using Tektronix TDS 2024B storage oscilloscope. The setup is shown in Fig. 2.

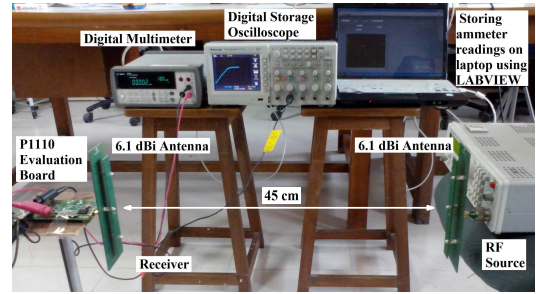


Fig. 2: Experimental setup

B. System parameters for numerical results

The parameter values for experimental validation as well as for charging time distribution are as follows. Super-capacitor related values: capacitance $C = 50$ mF, ESR $R = 0.16 \Omega$, maximum voltage $V_H = 3$ V, minimum required voltage $V_L = 2$ V. RF source related values: transmit power ($P_T \cdot G_T$) = 19.1 dBm, receiver antenna gain $G_R = 6.1$ dBi, operating frequency 915 MHz, charging distance $d = 0.45$ m, path loss exponent in Friis transmission equation (indoor) $\eta = 1.95$, received RF power 1.3 mW, harvesting efficiency 60% [14]. Thus, the harvested DC power $P = 0.8$ mW, initial charging current (using (12)) $I = 11.21$ mA, and initial voltage of the constant power source $V = 0.0714$ V (using $P = VI$). Hence, the time to charge from V_L to V_H , $T' = 156.25$ s.

C. Experimental results and verification of analytical model

Figs. 3(a) and 3(b) show a closely matched analytical and experimental results. Theoretically, the charging current should be very high at the beginning. However, the instrument has limitations of only recording finite values, and also the P1110 has its own surge-protection mechanism to protect the IC

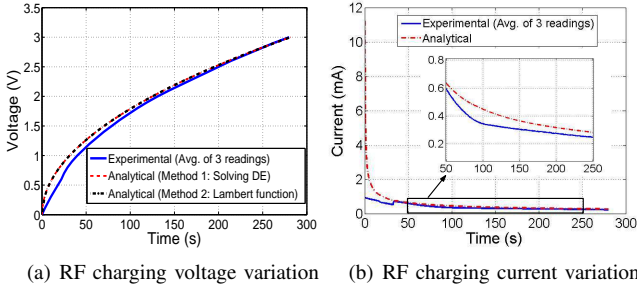


Fig. 3: Experimental validation of RF charging equations

from damage. At the start, there is a jump in the current and voltage around the time when the voltage across the super-capacitor reaches 0.7 V. Since the analysis did not account for surge-protection behavior, for verification of correctness of analysis the starting point of comparative data was taken when the voltage across the super-capacitor crossed 0.8 V. Root mean square error (RMSE) of the analytical voltage expression with respect to the mean of three experimental readings is 0.075, and the RMSE of the analytical current expression is 0.063, which are within the allowable upper limit 0.08 for a model to be considered as a good fit [16]. We consider these are acceptable as the analytical expressions for the sake of generality do not take into account the consumption by P1110 IC and assumes that the RF power received is constant.

V. RF CHARGING PERFORMANCE CASE STUDIES

We now provide the performance comparison of constant voltage charging and constant power charging based on the theoretical model in Section III-A. This is followed by validation of charging time distribution derived in Section III-B.

A. Constant voltage charging versus constant power charging

As noted in Section IV-B, the DC power from RF charging is quite low. With the same system parameters as in RF charging, it is difficult to experimentally monitor such low input power of a constant voltage source. Therefore, we resort to simulation based comparison with constant voltage charging. The circuit parameters (cf. Fig. 1(b)) taken were: source voltage $V_0 = 3$ V, resistance $R = 3$ Ω , initial current $I_0 = 1$ A, initial source power $\frac{V_0^2}{R} = 3$ W, and $C = 50$ mF.

The load in constant power case draws the same power throughout the charging duration, whereas with constant voltage case, the power drawn decreases with time (cf. Fig. 4(a)). In other words, the source voltage in constant power charging increases with time (cf. Fig. 4(b)). As a result, constant power charging is faster. Note that, constant power charging stops when the capacitor gets charged up to $V_H = 3$ V, i.e., at 0.2 s, whereas constant voltage charging takes up to 1 s.

The capacitor's voltage and current are plotted respectively in Figs. 4(c) and 4(d). The plots in constant power case appear to be linear because the input power is very high (3 W) in comparison with the maximum energy to be stored (0.225 J).

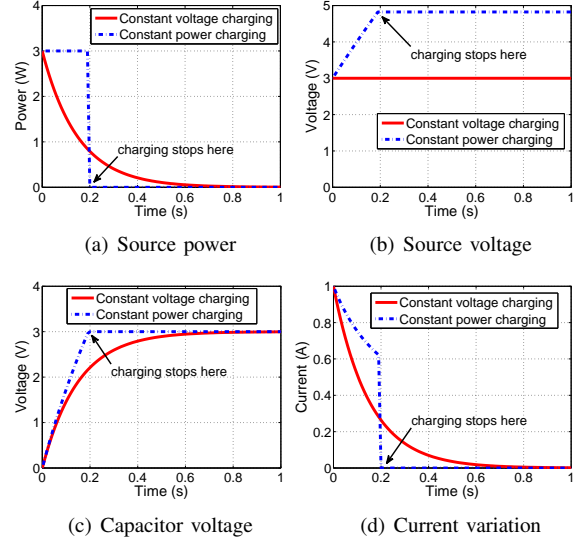


Fig. 4: Constant voltage versus constant power charging

B. Validation of RF charging time distribution

The following two cases of voltage distribution are taken:
 1) *Uniformly distributed residual voltage*: Here, V' is uniformly distributed between 2 V and 3 V, and its CDF is:

$$F_{V'}(x) = \begin{cases} 0 & x \leq 2 \\ (x - 2) & 2 \leq x \leq 3 \\ 1 & x \geq 3. \end{cases}$$

So, from (14), the CDF of RF charging time is:

$$\begin{aligned} F_{T_C}(t) &= 1 - F_{V'}(v) \\ &= \begin{cases} 0 & t \leq 0 \\ (3 - v) & 0 \leq t \leq T' \\ 1 & t \geq T' \end{cases} \end{aligned} \quad (17)$$

T' is the time to recharge a super-capacitor from 2 V to 3 V ($T' = T(3) - T(2) = 156.25$ s) and v is the initial residual voltage (cf. (15)). From (16), the charging time PDF is:

$$f_{T_C}(t) = \begin{cases} \frac{1}{C} \sqrt{\frac{P}{RZ''}} & 0 \leq t \leq T' \\ 0 & \text{otherwise} \end{cases} \quad (18)$$

because, $f_{V'}(x) = \begin{cases} 1 & 2 \leq x \leq 3 \\ 0 & \text{otherwise.} \end{cases}$

For simulation, 10^6 samples from the above uniform distribution were drawn and substituted in place of V' in (13), along with $V_H = 3$ V. The resultant was used to get the simulated CDF and PDF of RF charging time. The analytical CDF and PDF (respectively in (17) and (18)) are plotted against the simulated values in Fig. 5. The mean and variance of RF charging time in this case are respectively 83.40 s and 2040.70 s^2 . Fig. 5(a) shows that, although the simulation result on CDF matches closely with the analysis, it does not exactly match with the corresponding uniform fit in the interval $[0, 156.25]$. This is also clear from Fig. 5(b), which shows that the shape of PDF of RF charging time is different from the PDF of uniform distribution – which is a rectangular function.

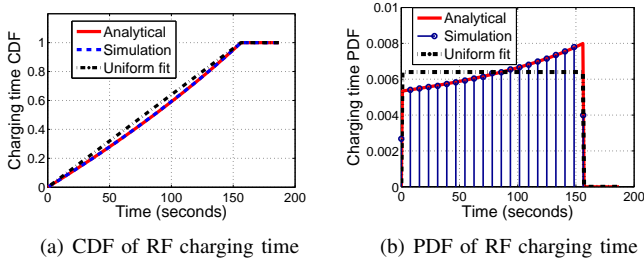


Fig. 5: Uniformly distributed residual voltage case

2) *Truncated normal distributed residual voltage*: Here V' has the truncated normal distribution with mean 2.5, variance 0.01, and $2 \leq V' \leq 3$. The CDF of V' is [17]:

$$F_{V'}(x) = \frac{\Phi\left(\frac{x-\mu}{\sigma}\right) - \Phi\left(\frac{2-\mu}{\sigma}\right)}{\Phi\left(\frac{3-\mu}{\sigma}\right) - \Phi\left(\frac{2-\mu}{\sigma}\right)} = \frac{\Phi\left(\frac{x-2.5}{0.1}\right) - 2.87 \times 10^{-7}}{0.9999994267}$$

where $\Phi(\cdot)$ is the CDF of the standard normal distribution. Hence, from (14),

$$F_{T_C}(t) = \begin{cases} 0 & t \leq 0 \\ 1 - \frac{\Phi\left(\frac{v-2.5}{0.1}\right) - 2.87 \times 10^{-7}}{0.9999994267} & 0 \leq t \leq T' \\ 1 & t \geq T'. \end{cases} \quad (19)$$

From (16), the PDF of charging time is:

$$f_{T_C}(t) = \begin{cases} \frac{\phi\left(\frac{v-2.5}{0.1}\right)}{0.9999994267} \left(\frac{1}{C} \sqrt{\frac{P}{RZ''}}\right) & 0 \leq t \leq T' \\ 0 & \text{otherwise} \end{cases} \quad (20)$$

where $\phi(\cdot)$ is the PDF of the standard normal distribution.

For simulation, 10^6 samples from the normal distribution with $\mu = 2.5$, $\sigma^2 = 0.01$ were drawn after neglecting the sample values outside the window [2, 3]. These values were used to substitute V' in (13). The resultant was used to get the simulated CDF and PDF of RF charging time, plotted in Fig. 6 against the respective analytical CDF and PDF in (19) and (20). The mean and variance of RF charging time in this case are 85.62 s and 244.63 s². Figs. 6(a) and 6(b), show a close match of the simulation results with the analysis. The CDF of charging time also fits very well with the corresponding truncated normal fit (cf. Fig. 6(a)) lying in the interval [0, 156.25], which is also clear from the fact that charging time follows truncated normal distribution (cf. Fig. 6(b)).

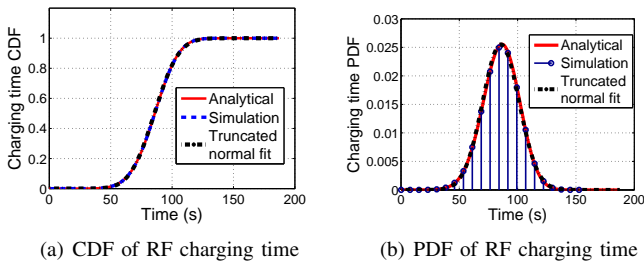


Fig. 6: Truncated normally distributed residual voltage case

Above observations with two chosen residual voltage distributions demonstrate that, although the RF charging time depends on the residual voltage, it does not necessarily follow exactly the same distribution as the underlying residual voltage.

VI. CONCLUDING REMARKS

We have shown that, RF charging involves practical aspects that go beyond constant power charging and is quite different from conventional constant voltage charging. To this end, RF charging equation and charging time distribution as a function of residual voltage distribution have been developed. The analytical model for RF charging has been experimentally validated. Further, nodal charging time distribution have been derived for uniform as well as truncated normal distributed residual voltage, which demonstrate that the charging time distribution does not necessarily follow the underlying residual voltage distribution. The analysis and the observations in this work are useful in evaluating the ability of RF harvesting assisted sustainable network operation.

As a future work, we intend to consider the RF charging profile for the enhanced super-capacitor model that incorporates the nonidealities attributed to substantial leakage currents.

REFERENCES

- [1] V. Raghunathan, A. Kansal, J. Hsu, J. Friedman, and M. B. Srivastava, "Design considerations for solar energy harvesting wireless embedded systems," in *Proc. IEEE ICNP*, Los Angeles, CA, USA, Apr. 2005.
- [2] S. Roundy, P. K. Wright, and J. Rabaey, "A study of low level vibrations as a power source for wireless sensor nodes," *Elsevier Computer Commun.*, vol. 26, no. 11, pp. 1131–1144, July 2003.
- [3] M. Weimer, T. Paing, and R. Zane, "Remote area wind energy harvesting for low-power autonomous sensors," in *Proc. IEEE Power Electronics Specialists Conf. (PESC)*, Jeju, Korea, June 2006.
- [4] J. A. Hagerty, F. B. Helmbrecht, W. H. McCalpin, R. Zane, and Z. B. Popovic, "Recycling ambient microwave energy with broadband rectenna arrays," *IEEE Trans. Microwave Theory and Techniques*, vol. 52, no. 3, pp. 1014–1024, Mar. 2004.
- [5] J. Gonzalez, A. Rubio, and F. Moll, "Human powered piezoelectric batteries to supply power to wearable electronic devices," *Intl. J. Soc. Materials Eng. Resources*, vol. 10, no. 1, pp. 34–40, 2002.
- [6] Z. A. Eu, W. K. G. Seah, and H.-P. Tan, "A study of MAC schemes for wireless sensor networks powered by ambient energy harvesting," in *Proc. ACM Intl. Conf. Wireless Internet*, Maui, HI, USA, Nov. 2008.
- [7] H. J. Visser, "Indoor wireless RF energy transfer for powering wireless sensors," *Radio Engineering*, vol. 21, no. 4, Dec. 2012.
- [8] S. De and R. Singhal, "Toward uninterrupted operation of wireless sensor networks," *IEEE Computer Mag.*, vol. 45, no. 9, pp. 24–30, Sep. 2012.
- [9] R. C. Shah, S. Roy, S. Jain, and W. Brunette, "Data mules: Modeling and analysis of a three-tier architecture for sparse sensor networks," *Elsevier Ad Hoc Networks*, vol. 1, no. 2, pp. 215–233, Sep. 2003.
- [10] L. Fu, P. Cheng, Y. Gu, J. Chen, and T. He, "Minimizing charging delay in wireless rechargeable sensor networks," in *Proc. IEEE INFOCOM*, Turin, Italy, Apr. 2013, pp. 2922–2930.
- [11] Z. Li, Y. Peng, W. Zhang, and D. Qiao, "J-RoC: A joint routing and charging scheme to prolong sensor network lifetime," in *Proc. IEEE ICNP*, Vancouver, BC, Canada, Oct. 2011, pp. 373–382.
- [12] J. Miller, "Electrical and thermal performance of the carbon-carbon ultracapacitor under constant power conditions," in *Proc. IEEE Veh. and Propul. Conf.*, Arlington, TX, USA, Sep. 2007, pp. 559–566.
- [13] M. W. Verbrugge and P. Liu, "Analytic solutions and experimental data for cyclic voltammetry and constant-power operation of capacitors consistent with HEV applications," *J. Electrochem. Soc.*, vol. 153, no. 6, pp. A1237–A1245, May 2006.
- [14] Powercast P1110 powerharvester receiver datasheet. [Online]. Available: <http://www.powercastco.com/PDF/P1110-datasheet.pdf>
- [15] E. W. Weisstein, "Lambert W-Function," From MathWorld – A Wolfram Web Resource. [Online]. Available: <http://mathworld.wolfram.com/LambertW-Function.html>
- [16] D. Hooper, J. Coughlan, and M. R. Mullen, "Structural equation modeling: Guidelines for determining model fit," *Electronic J. Business Research Methods*, vol. 6, no. 1, Apr. 2008.
- [17] N. L. Johnson, S. Kotz, and N. Balakrishnan, "Continuous univariate distributions, vol. 1," *John Wiley and Sons*, 1994.